CAME 55
STEADY STATE AND THERMOELASTIC ANALYSIS OF A FUNCTIONALLY GRADED ROTATING DISK

M.M. Shahzamanian[1,2*], B.B. Sahari [1,2], M. Bayat [3], F. Mustapha [4], Z.N. Ismarrubie [1], A. Shahrjerdi [1]
[1] Mechanical and Manufacturing Engineering Department, Universiti Putra Malaysia.
[2] Institute of Advance Technology (ITMA), Universiti Putra Malaysia.
[3]Mechanical Engineering Department, University of Malaya.
[4]Aerospace Engineering Department, Universiti Putra Malaysia.
*Email: mmshahzamanian@yahoo.com

ABSTRACT
In this paper, the steady state and thermoelastic analysis of a hollow functionally graded (FG) axisymmetric rotating disk is carried out. The inner and outer surfaces of FG disks are considered metal and ceramic respectively. The material properties of FG disk are assumed to be represented by a power-law distribution along the radial direction. Temperature distributions of FG disk are obtained by three methods, namely, using ANSYS parametric design language (APDL), developed finite element program and analytical solution. Thermal stress and thermal strain of FG disk are given by developed finite element program. The results show that the same temperature distributions are obtained.

Keywords: *functionally graded material, thermoelastic analysis, steady state, rotating disk.*

INTRODUCTION
Functionally Graded Materials (FGMs) are those which the volume fraction of two or more materials is varied smoothly and continuously as a function of position along certain dimension(s) of the structure from one point to the other [1, 2]. Bayat et al. [3-4] presented the thermoelastic analysis of FG rotating disk by considering the small and large deflection. Also they have analyzed the FG rotating disk as variable thickness. Zenkour [5] analyzed the stress distribution of rotating composite structures of functionally graded solid disks**.** Numerical results for displacement and stress in two types of composite rotating disks are considered. The effects of some parameters on results are investigated. Shahzamanian et al. [6] simulated FG brake disks by using APDL. They have investigated five types of FG brake disks in term of contact status and deflection. Jabbari et al. [7] analyzed the thermoelastic analysis of short thick hollow FG cylinder by using Bessel function for two types of boundary condition.

In this study, a FG hollow axisymmetric rotating disk with inner radius, r_i outer radius, r_o thickness, h and axisymmetric with respect to z-axis is considered. The material properties of FG rotating disk are assumed by power-law distribution. Inner surface is full-metal and outer radius is full-ceramic. The temperature distribution of rotating disk is obtained by three methods of using ANSYS software, analytical solution and developed finite element program. Thermal stress and thermal strain of FG rotating disk are obtained by developed finite element method.

GRADATION RELATION
The material properties of FG rotating disk are considered as the following relation along the radial direction [7].

$$P(r) = P_{\bullet} r^{m_3} \tag{1}$$

where $P_{\bullet}$ and m are material parameters and P is the material property at radius of r. The variation of thermal conductivity, modulus of elasticity and thermal expansion are assumed to vary according to gradation of equation (1).

The variation of non-dimensional thermal conductivity (K / K_o) along the non-dimensional radius (r / r_o) is shown in Figure 1.

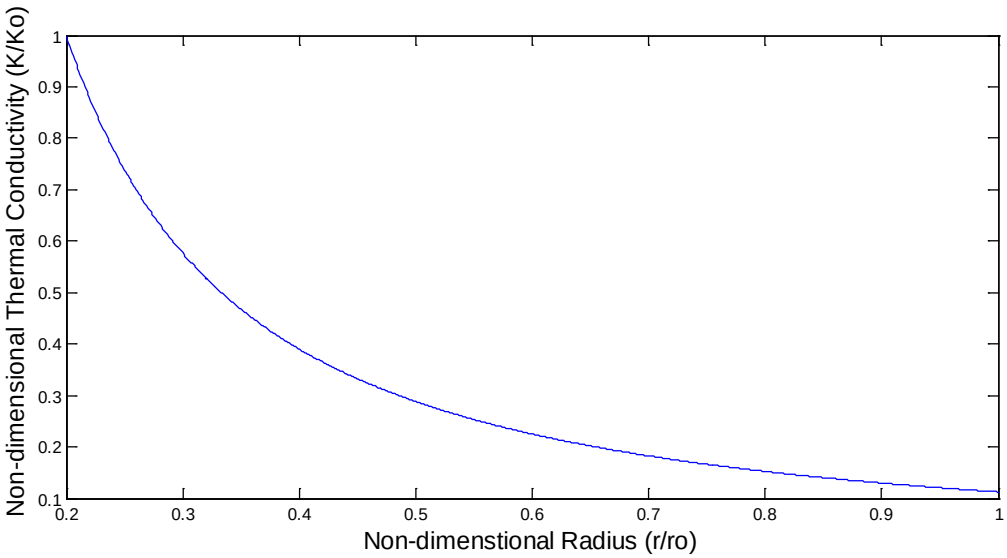

Figure 1: Variation of thermal conductivity versus non-dimensional radius

THERMAL BOUNDARY COUNDITION

At the inner surface ($\frac{r}{r_o} = 0.2$) temperature value is zero ($T = 0^\circ C$) and at the outer surface ($\frac{r}{r_o} = 1.0m$) temperature value is one hundred centigrade ($T = 100^\circ C$).

METHODOLOGY

In this case, temperature distribution of FG rotating disk is presented by three methods by the names of 1) ANSYS parametric design language (APDL), 2) developed finite element program and 3) analytical solution.

1) ANSYS PARAMETRIC DESIGN LANGUAGE (APDL)

For the purpose of using ANSYS parametric design language (APDL), the FG rotating disk is divided into two hundred elements as shown in Figure 2. To obtain the temperature distribution plane42 element is applied. The thermal conductivity of FG rotating disk is evaluated at the mean radius of each element. Increasing the number of the elements improves the accuracy of the results [6].

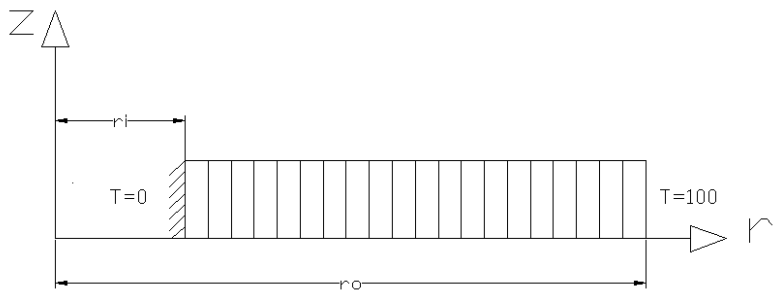

Figure 2: Mesh division of FG rotating disk in ANSYS software.

2) DEVELOPED FINITE ELEMENT PROGRAM

The temperature distribution of FG rotating disk can be written as:

$$\frac{1}{r}\left(\frac{\partial}{\partial r}\right)\left(rk\left(r\right)\frac{\partial T}{\partial r}\right)+\frac{\partial}{\partial z}\left(k\left(r\right)\frac{\partial T}{\partial z}\right)=0 \qquad (2)$$

By expanding equation 2, we have:

$$\left(\left[\frac{k(r)}{r}+k'(r)\right]\frac{\partial T}{\partial r}+k(r)\frac{\partial^2 T}{\partial r^2}\right)+k(r)\frac{\partial^2 T}{\partial z^2}=0 \tag{3}$$

$$\left[\frac{1}{r}+\frac{k'(r)}{k(r)}\right]\frac{\partial T}{\partial r}+\frac{\partial^2 T}{\partial r^2}+\frac{\partial^2 T}{\partial z^2}=0 \tag{4}$$

Equation 7 can be found from equation 1:

$$\frac{k'(r)}{k(r)}=\frac{m_3}{r} \tag{5}$$

By substituting equation 5 into equation 4, we have:

$$\left[\frac{1}{r}+\frac{m_3}{r}\right]\frac{\partial T}{\partial r}+\frac{\partial^2 T}{\partial r^2}+\frac{\partial^2 T}{\partial z^2}=0 \tag{6}$$

$$\frac{\partial^2 T}{\partial r^2}+\frac{1}{r}\frac{\partial T}{\partial r}+\frac{\partial^2 T}{\partial z^2}+\left(\frac{m_3}{r}\right)\frac{\partial T}{\partial r}=0 \tag{7}$$

By applying the weighted residual method, the element matrix integral becomes:

$$\int_{\Omega}\omega\left(\frac{\partial^2 T}{\partial r^2}+\frac{1}{r}\frac{\partial T}{\partial r}+\frac{\partial^2 T}{\partial z^2}+\left(\frac{m_3}{r}\right)\frac{\partial T}{\partial r}\right)d\Omega \tag{8}$$

Here, ω is weighted residual. The equation 8 can be written as:

$$\int_{\Omega}\omega\left(\frac{1}{r}\frac{\partial}{\partial r}\left(\frac{\partial T}{\partial r}\right)+\frac{\partial^2 T}{\partial z^2}+\left(\frac{m_3}{r}\right)\frac{\partial T}{\partial r}\right)d\Omega \tag{9}$$

The domain integral can be expressed as axisymmetric cylindrical which is shown in Equation 10.

$$\begin{aligned}&\int_{\Omega}\omega\left(\frac{1}{r}\frac{\partial}{\partial r}\left(\frac{\partial T}{\partial r}\right)+\frac{\partial^2 T}{\partial z^2}+\left(\frac{m_3}{r}\right)\frac{\partial T}{\partial r}\right)d\Omega\\&=2\pi\int_r\int_z r\left(\omega\left(\frac{1}{r}\frac{\partial}{\partial r}\left(\frac{\partial T}{\partial r}\right)+\frac{\partial^2 T}{\partial z^2}+\left(\frac{m_3}{r}\right)\frac{\partial T}{\partial r}\right)\right)dr\,dz\end{aligned} \tag{10}$$

Equation 10 can be rewritten into equation 11,

$$2\pi\int_r\int_z \omega\left(\frac{\partial}{\partial r}\left(\frac{\partial T}{\partial r}\right)+r\frac{\partial^2 T}{\partial z^2}+m_3\frac{\partial T}{\partial r}\right)dr\,dz \tag{11}$$

The weak formulation of the first two terms in Eqn. 11 using the integration by parts is replaced in Eqn. 13:

$$2\pi\int_r\int_z r\left(-\frac{\partial\omega}{\partial r}\frac{\partial T}{\partial r}+\frac{\partial\omega}{\partial z}\frac{\partial T}{\partial z}+\frac{m_3}{r}\frac{\partial T}{\partial r}\right)dr\,dz \tag{12}$$

In this method axisymmetric triangular element is used. Eighty axisymmetric elements are applied. The mesh division by this element is shown in Figure 3. The element matrix for axisymmetric triangular element can be expressed by equation 13.

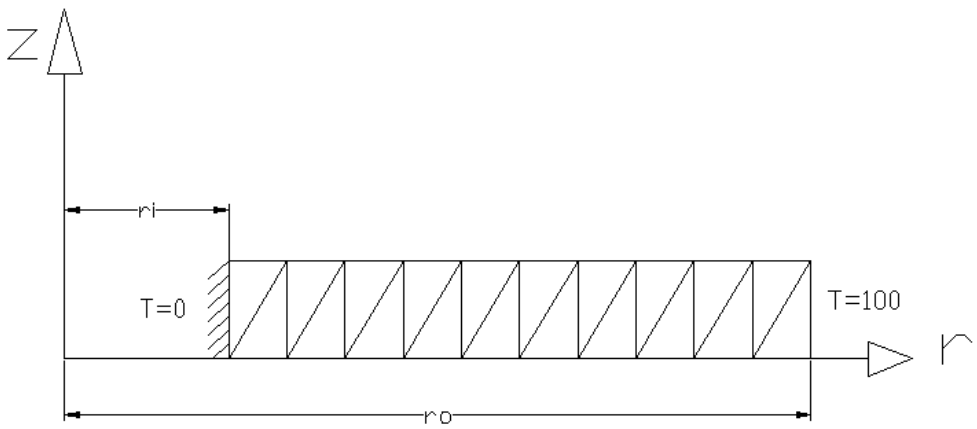

Figure 3: Mesh division of FG rotating disk by axisymmetric triangular element.

$$[k]=2\pi\int_z\int_r\left\{r\left(-\begin{Bmatrix}\frac{\partial H_1}{\partial r}\\ \frac{\partial H_2}{\partial r}\\ \frac{\partial H_3}{\partial r}\end{Bmatrix}\begin{Bmatrix}\frac{\partial H_1}{\partial r} & \frac{\partial H_2}{\partial r} & \frac{\partial H_3}{\partial r}\end{Bmatrix}-\begin{Bmatrix}\frac{\partial H_1}{\partial z}\\ \frac{\partial H_2}{\partial z}\\ \frac{\partial H_3}{\partial z}\end{Bmatrix}\begin{Bmatrix}\frac{\partial H_1}{\partial z} & \frac{\partial H_2}{\partial z} & \frac{\partial H_3}{\partial z}\end{Bmatrix}+\frac{m_3}{r}\begin{Bmatrix}H_1\\ H_2\\ H_3\end{Bmatrix}\begin{Bmatrix}\frac{\partial H_1}{\partial r} & \frac{\partial H_2}{\partial r} & \frac{\partial H_3}{\partial r}\end{Bmatrix}\right)\right\}dzdr \tag{13}$$

where, H_1, H_2 and H_3 are shape functions of axisymmetric triangular element. To find the vector of temperature (T), the equation 14 should be solved.

$$[k]\{T\}=\{F\} \tag{14}$$

where, matrix of F is the force vector.

3) ANALYTICAL SOLUTION

In this case, temperature distribution of inner and outer surfaces are $0^\circ C$ and $100^\circ C$, respectively. Due to this fact, variation of temperature is only in radial direction. Therefore, equation 15 can be found by neglecting the terms in thickness direction of equation 2.

$$\frac{\partial^2 T}{\partial r^2}+\left(\frac{m_3+1}{r}\right)\frac{\partial T}{\partial r}=0 \tag{15}$$

$$r^2\frac{\partial^2 T}{\partial r^2}+Ar\frac{\partial T}{\partial r}=0 \tag{16}$$

where $A=m_3+1$. By considering, $r=e^t$ or $t=\ln r$ we have:

$$\frac{dT}{dr}=\frac{dT}{dt}\frac{dt}{dr}=\frac{dT}{rdt} \tag{17}$$

$$\frac{d^2T}{dr^2}=\frac{d}{dr}\left(\frac{dT}{dr}\right)=\frac{d}{dr}\left[\frac{dT}{dt}\frac{1}{r}\right]=\frac{d}{dr}\left[\frac{dT}{dr}e^{-t}\right]=\frac{d\left[\frac{dT}{dr}e^{-t}\right]}{dt}\frac{dt}{dr}=\frac{d\left[\frac{dT}{dr}e^{-t}\right]}{dt}\frac{1}{r}=\left[\frac{d^2T}{dt^2}e^{-t}-\frac{dT}{dt}e^{-t}\right]e^{-t} \tag{18}$$

$$\frac{d^2T}{dt^2}e^{-2t}-\frac{dT}{dt}e^{-2t}+Ae^{-t}\frac{dT}{dr}e^{-t}=\frac{d^2T}{dt^2}e^{-2t}-\frac{dT}{dt}e^{-2t}+A\frac{dT}{dr}e^{-2t}=\frac{d^2T}{dt^2}e^{-2t}+(A-1)\frac{dT}{dt}e^{-2t}=0 \tag{19}$$

$$T''+(A-1)T'=0 \tag{20}$$

$$\frac{d\left(\frac{dT}{dt}\right)}{dt}=(1-A)\frac{dT}{dt} \tag{21}$$

By considering $\frac{dT}{dt} = X$, we have:

$$X = e^{(1-A)t+c_1} \tag{22}$$

where c_1 is one constant.

$$T'(t) = e^{(1-A)t+c_1} \tag{23}$$

$$T(t) = \frac{e^{(1-A)t+c_1}}{(1-A)} + c_2 \tag{24}$$

$$T(r) = \frac{e^{(1-A)\ln r+c_1}}{(1-A)} + c_2 \tag{25}$$

Finally the temperature distribution becomes as follow:

$$T(r) = \frac{e^{-m_3 \ln r+c_1}}{-m_3} + c_2 \tag{26}$$

c_1 and c_2 are constant which are found by applying the boundary condition.

THERMAL STRESS AND THERMAL STRAIN RELATIONS

The formulation of thermal stress and thermal strain in FG rotating disk are given in equations 27-28, respectively.

$$\sigma^T = \frac{E(r)}{(1-\upsilon^2)}\left[(1+\upsilon)\alpha(r)T(r)\right] \tag{27}$$

$$\varepsilon^T = \alpha(r)T(r) \tag{28}$$

where, $E(r) = E_{\bullet} r^{m1}$ and $\alpha(r) = \alpha_{\bullet} r^{m2}$. $\alpha_{\bullet}, m_2, E_{\bullet}$ and m_1 are material parameters and $\upsilon = 0.3$.

NUMERICAL RESULTS AND DISCUSSION

In this case, inner and outer radiuses and thickness of hollow FG brake disk are $r_i = 0.2m$ $r_o = 1.0m$ and $h = 0.1m$ respectively. The angular velocity of disk is $\omega = 1000 rad/s$. The material properties are shown in Table 1 [7].

Table 1: Material properties

Material properties	$E\ (GPa)$	υ	$\alpha\ (\frac{1}{K})$	$K\ (\frac{W}{mK})$
Outer surface, Ceramic	117	0.3	7.11×10^{-6}	2.036
Inner surface, Metal	66.2	0.3	10.3×10^{-6}	18.1

The temperature distribution of FG disk is obtained by three methods of using ANSYS parametric design language (APDL), developed finite element program and analytical solution as shown in Figure 4.

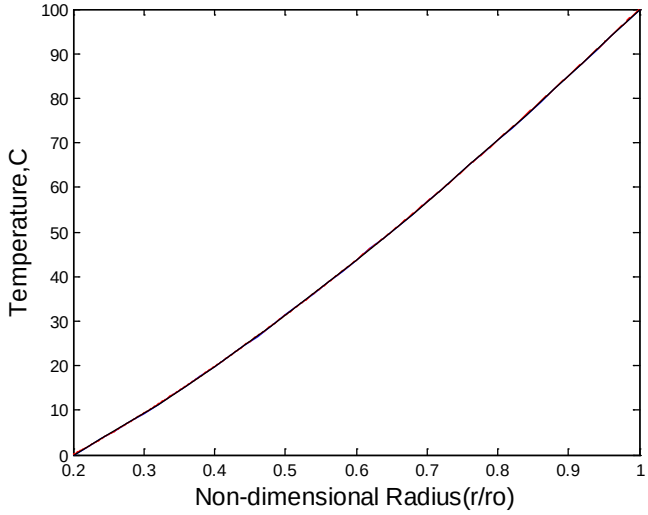

Figure 4: Temperature distribution by three methods

From Figure 4, it can be seen that temperature distribution obtained from all of the three methods are exactly same. Thermal strain and thermal stress of FG rotating disk is demonstrated in Figures 5-6, respectively. Both thermal strain and thermal stress are presented by developed finite element program.

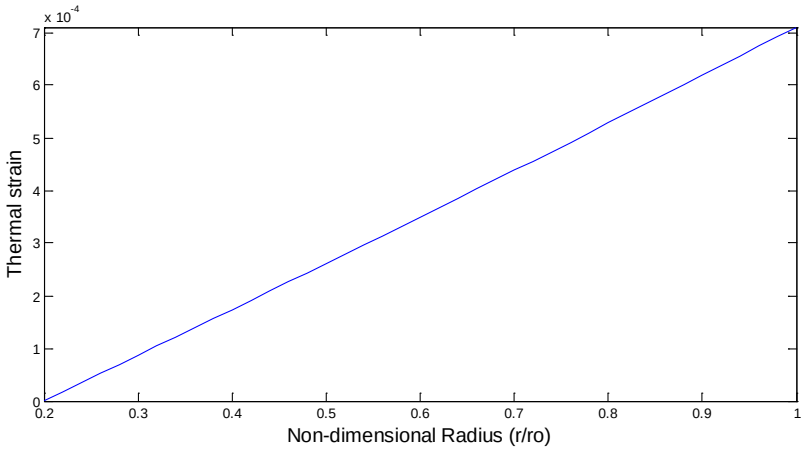

Figure 5: Variation of thermal strain versus non-dimensional radius

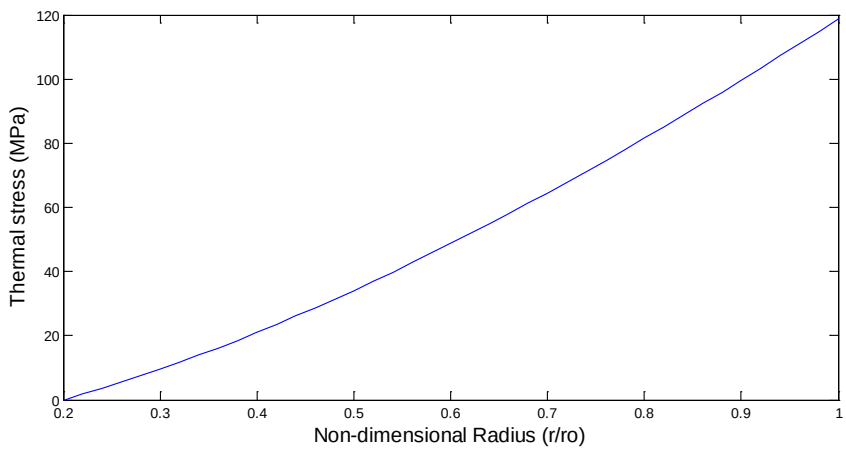

Figure 6: Variation of thermal stress versus non-dimensional radius

From Figure 5-6, it can be noted that the maximum thermal strain and thermal stress occur at the outer surface. The values of maximum thermal strain and thermal stress are 0.000711 and $118.8\ MPa$ respectively.

CONCLUSION

Temperature distribution of a hollow FG rotating disk is analyzed. The material properties of FG axisymmetric rotating disk vary along the radial direction. The inner surface of disk is assumed as full-metal and the outer surface is considered as full-ceramic. The value of temperature at the inner and outer surfaces are $0^{\circ}C$ and $100^{\circ}C$, respectively. Three methods were used, namely, 1) using ANSYS parametric design language (APDL), 2) using developed finite element program and 3) using analytical solution to obtain the temperature distribution. Thermal strain and thermal stress are presented for the method of using the developed finite element program. It is seen that the temperature distribution obtained by these methods are exactly same. It can be concluded that in steady thermal analysis of FG rotating disk these three methods are worthwhile.

REFERENCES

[1] Suresh, S. (1998) Mortensen, A, Fundamentals of functionally graded materials. London: Institute of Materials (IOM) Communications Limited, 1998.
[2] Reddy, J.N. (2000) Analysis of functionally graded plates. International Journal of Numerical Methods in Engineering 47, 663–684.
[3] Bayat, M, Saleem, M, Sahari, B.B, Hamouda, A.M.S, Mahdi, E. (2007) Thermo elastic analysis of a functionally graded rotating disk with small and large deflections. Thin-Walled Structures 45, 677–691.
[4] Bayat, M, Saleem, M, Sahari, B.B, Hamouda, A.M.S, Mahdi, E. (2008) Analysis of functionally graded rotating disks with variable thickness. Mechanics Research Communications 35, 283–309.
[5] A.M. Zenkour. (2009) Stress distribution in rotating composite structures of functionally graded solid disks. 209, 3511-3517.
[6] Shahzamanian, M.M, Sahari, B.B, Bayat, M, Mustapha, F, Ismarrubie, Z.N. (2010) Finite element analysis of thermoelastic contact problem in functionally graded axisymmetric brake disks. Composite Structures 92, 1591–1602.
[7] Jabbari, M, Bahtui, A, Eslami, M.R. (2009) Axisymmetric Mechanical and Thermal Stresses in Thick Short Length FGM Cylinders. International journal of pressure vessel and piping 86, 296-306.